Advances in Geo-Energy Research

Vol. 6, No. 2, p. 169-176, 2022

Original article

Characteristics of gas-oil contact and mobilization limit during gas-assisted gravity drainage process

Debin Kong[1,2]*, Jidong Gao[1,2], Peiqing Lian[3], Rongchen Zheng[3], Weiyao Zhu[1,2], Yi Xu[4]

[1]*School of Civil and Resources Engineering, University of Science and Technology Beijing, Beijing 100083, P. R. China*

[2]*Institute of Applied Mechanics, University of Science and Technology Beijing, Beijing 100083, P. R. China*

[3]*SINOPEC Petroleum Exploration and Production Research Institute, Beijing 100083, P. R. China*

[4]*School of Engineering, University of Glasgow, Glasgow G12 8QQ, Scotland, UK*

Keywords:
Gas-assisted gravity drainage
mobilization limit
gas-oil contact
interface migration rate

Cited as:
Kong, D., Gao, J., Lian, P., Zheng, R, Zhu, W., Xu, Y. Characteristics of gas-oil contact and mobilization limit during gas-assisted gravity drainage process. Advances in Geo-Energy Research, 2022, 6(2): 169-176.
https://doi.org/10.46690/ager.2022.02.08

Abstract:
Gravity can reduce the instability of the gas-oil contact that is caused by gas channeling in locations with low flow resistance, such as high-permeability layers, macropores, and fractures during the gas-assisted gravity drainage process. Herein, the microscopic forces during the gas-assisted gravity drainage process were analyzed and combined with the capillary model to study the occurrence boundary of gas-assisted gravity drainage process, and the characteristics of the gas-oil contact in the gas-assisted gravity drainage process was discussed. The results show that free gravity drainage occurs only in pores where a certain height of the oil column and pore radius are reached. Furthermore, the lower the oil-gas interface migration rate, the easier free gravity drainage occurs. In other scenarios, additional gas injection is required. During the gas-assisted gravity drainage process, the gas-oil contact moves down stably as a transition. The width of the transition zone and the available pore radius are related to the gas-oil contact migration rate and the oil viscosity; the smaller the gas-oil contact migration rate and the lower the oil viscosity, the smaller pore throat can be involved in mobilization. Optimizing the gas injection rate and reducing the oil viscosity can delay the gas channeling maturity time, which is beneficial for the realization of the gas-assisted gravity drainage process. Finally, a method considering micropore heterogeneity is established for determining the critical gas injection rate, while the mainstream pore throat can be involved in mobilization and the gas-oil contact can be stabilized at the same time. The method of determining the critical gas injection rate can help researchers and reservoir engineers to better understand and implement the gas-assisted gravity drainage process.

1. Introduction

Gas flooding is one of the main strategies to enhance oil recovery, which includes continuous gas injection and water-alternating-gas (WAG) (Lv et al., 2015; Kong et al., 2021a). The original intention of WAG is to solve the gas override effect, but it is still a method that violates the natural phenomenon of gravity separation. To solve this problem, scholars have derived a method that involves gas-assisted gravity drainage (GAGD) development technology (Rao et al., 2004; Al-Mudhafar et al., 2017; Wang et al., 2019; Chen et al., 2020). A vertical well is used to inject gas on top of the oil layer, and the density difference between the injected gas and the oil in the oil layer forms an obvious gas-oil contact (GOC). The gas-liquid interface can be maintained by controlling the gas injection rate. The stable interface moves downward and expands laterally, and then gradually pushes the oil to the horizontal oil well above the oil-water interface (Kulkarni and Rao, 2006). The combination of theoretical research and field practice (Al-Mudhafar et al., 2017) revealed that the GAGD can inhibit viscous fingering, expand the sweep volume, improve the microscopic oil displacement efficiency, and significantly improve the ultimate oil recovery. Hagoort

Yandy Scientific Press

*Corresponding author.
E-mail address: kongdb@ustb.edu.cn (D. Kong); gaojd2021@163.com (J. Gao); lianpq.syky@sinopec.com (P. Lian); zhengrc.syky@sinopec.com (R. Zheng); weiyaook@sina.com (W. Zhu); 2421380x@student.gla.ac.uk (Y. Xu).

Received March 7, 2022; revised March 18, 2022; accepted March 19, 2022; available online March 22, 2022.

(1980) defined gravity drainage as a recovery process in which gravity is the main driving force and gas replaces void volume, which constitutes a gas/oil displacement process dominated by gravity. Free fall gravity drainage (FFGD) means that crude oil relies on the movement of gravity free fall to reach the production well, in order to obtain the highest recovery rates (Hasanzadeh et al., 2021). However, crude oil is quickly produced from high-permeability areas (such as fractures), and a large proportion of low-permeability areas cannot be swept during FFGD. In fact, the crude oil in the matrix and small pores can only be extracted by the imbibition effect dominated by capillary force and gravity. At present, the commonly used method of gravity drainage is forced gravity drainage (Hasanzadeh et al., 2021), which uses pumps to control the production speed or pressure to inject gas at the top of the oil layer during the oilfield development process.

The stable migration of GOC during GAGD can yield a higher swept volume, which is much higher than that of unstable displacement. The stability of GOC is related to the reservoir geological conditions, fluid properties and injection rate. The flow influenced by gravity is usually investigated by the segregated flow theory. The motion of the phase interface in the porous flow influenced by gravity has been fully described. Dietz (1953) first studied the piston displacement characteristics for water flooding in a tilted reservoir, and established stable oil-water interface under gravity-dominated conditions. Outmans (1962) considered the influence of oil-water interfacial tension on the interface and defined the interface stability problem. Sheldon and Fayers (1962) deduced the fluid interface motion equation of a tilted reservoir, which considered the gravity terms related to the reservoir dip and the curvature of the fluid interface. Moreover, the approach of average saturation developed by Dake (1978) could predict the motion of interface in the tilted reservoir. Colla (2014) proposed an analytical calculation method for the motion of the two-phase interface to calculate the position, dip and velocity of the two-phase interface in a tilted reservoir. This method introduces the Lambertian W function to calculate the dip of the two-phase interface. Reservoir heterogeneity promotes the formation of gas channeling and reduces the stability and macroscopic swept volume of the gas flooding front.

The gas injection rate affects the stability of GOC, as it determines whether GOC is uniformly displaced downward or viscous fingering will occur. The experimental results with different gas injection rates for GAGD showed that, when the oil and gas front was stable, the higher the injection rate, the better the oil recovery (Meszaros et al., 1990; Mahmoud and Rao, 2017). The maximum gas injection rate at which a stable GOC front can be obtained is called the critical gas injection rate. S. Hill and F. Inst. P. (1952) first proposed the critical gas injection rate for interface stability in homogeneous oil reservoirs, and many scholars (Dietz, 1953; Dumore, 1964) subsequently made certain modifications on this basis. However, the influence of microscopic pore heterogeneity on the interface stability was not considered.

Analyzing the force balance can help to understand the displacement mechanism in the flowing system of interest (Rahman et al., 2017; Namba et al., 2018). Based on the force mechanics of microscopic residual oil in the flow process (Stephen et al., 2001; Liu et al., 2017), the distribution of residual oil is mainly affected by the displacement force of injected phase, the capillary force caused by two-phase interfacial tension, the gravity caused by two-phase density, and the fluid viscous force. Displacement force is always the driving force for the oil flow. Whether capillary force and gravity can be the driving force depends on whether their direction is consistent with the flow direction. The viscous force is the internal friction of the fluid, which is always the flow resistance. Gravity plays a dominant role in oil recovery during the process of GAGD (Grattoni et al., 2001; Raeini et al., 2014; Khorshidian et al., 2018); the force of gravity increases the stability of gas flooding front. Kong et al. (2020) obtained the equivalent gravity and found the GAGD process to be dominated by gravitational forces. Gravity improves the gas flooding front stability and it provides hydraulic pressure to overcome the capillary and viscous force (Khorshidian et al., 2018; Kong et al., 2021b; Yu et al., 2021). Wang et al. (2019) conducted the force analysis of resistance and driving forces in a single capillary tube during GAGD, and found that, when the capillary diameter reduces to a certain value, the oil flow resistance of crude oil will be stronger than gravity, and a large driven pressure difference is required for drainage. However, the use of a bundle of capillary tubes to represent a field-scale reservoir also has some deviations from reality. For example, the capillary model does not consider the connectivity of individual pores and the entrapment of oil. Nonetheless, it can provide us with a level of insight into the field-scale operating parameters.

The aims of this paper are to determine where the current stability criteria apply to the GAGD process to theoretically provide basic design data for GAGD. It also contributes to our understanding of the capillary, viscous and gravity forces acting in the GAGD process. Therefore, this paper firstly conducts force balance analysis during GAGD, investigates the current stability criteria of GAGD in the capillary model and analyzes the GOC characteristics during the GAGD process, and finally proposes a calculation method for the critical gas injection rate to determine where the current stability criteria apply to the GAGD process, which method considers the microscopic pore heterogeneity.

2. Free fall gravity drainage in a capillary tube

As shown in Fig. 1, the force balance analysis during GAGD indicates that the fluids in a capillary are dominated by five kinds of force: the gravity force of gas and oil, the viscous resistance between fluid and capillary tube, the capillary force between gas phase and oil phase, the buoyancy of the oil phase due to the gas-oil density difference, and the displacement force of injected gas. Here, gas is the nonwetting phase, and oil is the wetting phase. It is assumed that the oil length in the capillary tube is L.

The total gravity force of oil G can be calculated as:

$$G = m_o g = \pi r^2 \rho_o L g \tag{1}$$

Table 1. Fluid parameters in Jilin oilfield.

Parameter	ρ_o (kg/m^3)	ρ_g (kg/m^3)	μ_o (mPa·s)	μ_g (mPa·s)	σ (N/m)	θ (°)
Value	850	14.01	1.88	0.0233	13.33×10^{-3}	32

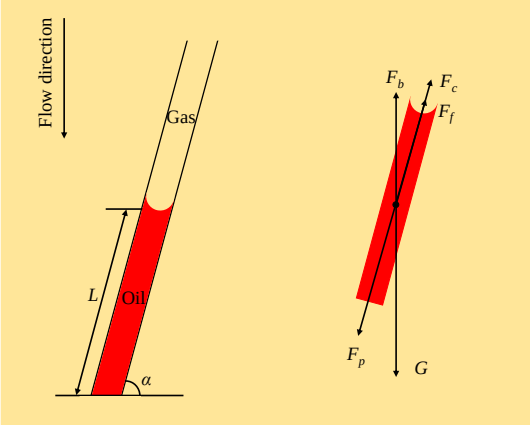

Fig. 1. Schematic diagram of concurrent GAGD into an oil-saturated capillary tube and subsequent force balance analysis.

where m_o denotes the mass of oil in the capillary tube, r denotes the capillary tube radius, ρ_o denotes the oil density, and g denotes the gravity acceleration.

The capillary force between the gas and oil F_c can be expressed as:

$$F_c = \pi r^2 \frac{2\sigma\cos\theta}{r} = 2\pi r\sigma\cos\theta \tag{2}$$

where σ indicates oil and gas interface tension, and θ is wetting angle.

It is assumed that the viscosity of the gas μ_g is negligible compared to the viscosity of the oil, and the viscous resistance between the oil and the capillary tube F_f can be expressed as:

$$F_f = \pi\mu_o vL \tag{3}$$

where μ_o represents oil viscosity, and v is GOC migration rate.

The buoyancy of the oil phase due to the oil-gas density difference F_b can be calculated as:

$$F_b = \rho_g g\pi r^2 L \tag{4}$$

where ρ_g represents the gas density.

The displacement force F_p of the injected gas can be expressed as:

$$F_p = 8\pi r^2\Delta p \tag{5}$$

where Δp represents the displacement pressure difference.

During the process of GAGD, the driving forces include the gravity force of gas and oil, and the displacement force of injected gas. The resistance forces include the viscous resistance between fluid and capillary tube, the capillary force between gas phase and oil phase, and the buoyancy of the oil phase due to the gas-oil density difference (Grattoni et al., 2001; Raeini et al., 2014; Khorshidian et al., 2018). According to Newton's second law, the force p_F in the direction of motion of the oil column in the capillary can be obtained as:

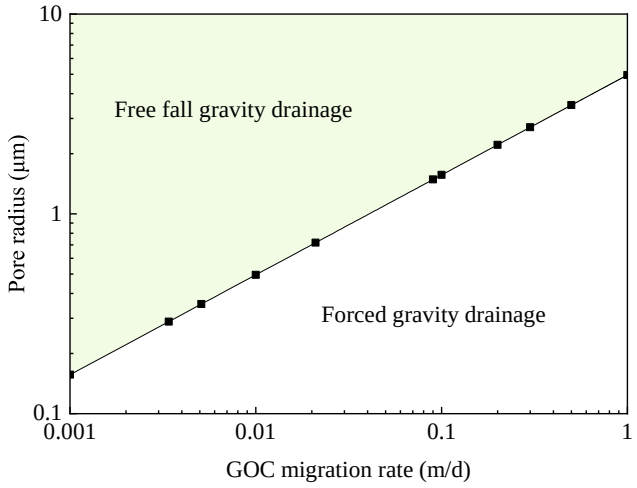

Fig. 2. Relationship between GOC migration rate and critical pore radius.

$$\begin{aligned} p_F &= \frac{F_p + G\sin\alpha - (F_c + F_f + F_b\sin\alpha)}{\pi r^2} \\ &= \Delta p + (\rho_o - \rho_g)gL\sin\alpha - \frac{8\mu_o vL}{r^2} - \frac{2\sigma\cos\theta}{r} \end{aligned} \tag{6}$$

where α denotes the angle between the capillary tube and the horizontal plane.

The oil column can be mobilized because the driving force is greater than resistance, that is, $p_F < 0$. It can be determined that FFGD occurs according to the definition when the displacement pressure difference Δp is 0 and gravity plays a dominant role. Therefore, Eq. (6) can be transformed to calculate the minimum oil column length for FFGD at a certain equivalent oil column radius, which can be expressed as:

$$L > \frac{2\sigma\cos\theta}{(\rho_o - \rho_g)gr^2\sin\alpha - 8\mu_o v} \tag{7}$$

Eq. (7) requires $(\rho_o - \rho_g)gr^2\sin\alpha - 8\mu_o v > 0$, that is, the equivalent oil column radius should be greater than the critical pore radius, where a certain value can be calculated as:

$$r > \sqrt{\frac{8\mu_o v}{(\rho_o - \rho_g)g\sin\alpha}} \tag{8}$$

Therefore, FFGD can only occur if the oil column reaches the minimum length and minimum radius, calculated by Eqs. (7) and (8), respectively.

Taking Jilin oilfield as an example (Chen et al., 2020), the reservoir temperature is 100 °C, the pressure is 15 MPa, the injection gas is air, and the angle between the flow direction and the horizontal direction is 60°. The fluid parameters in Jilin oilfield is shown in Table 1.

Accordingly, the relationship curve between the critical GOC migration rate and the critical pore radius can be obtained, as shown in Fig. 2. FFGD can only occur in the

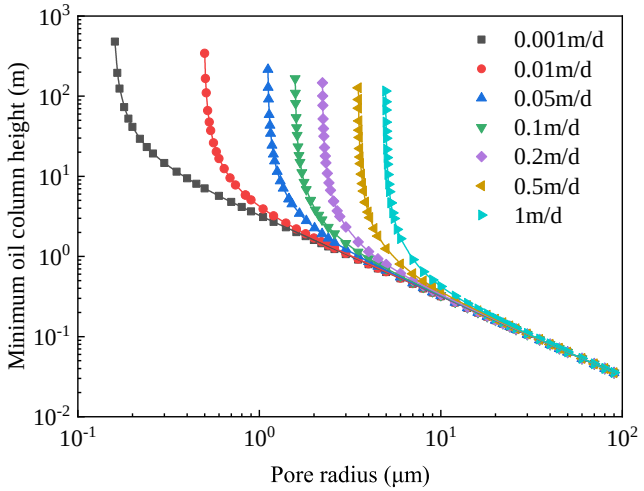

Fig. 3. Minimum oil column height at different pore radii.

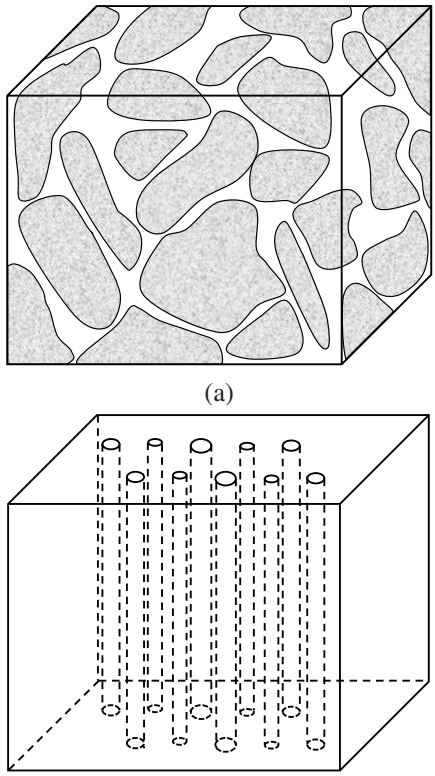

Fig. 4. Schematic diagram of porous media in a reservoir (a) and the classical capillary model (b).

pores greater than the critical pore radius at a certain GOC migration rate. Otherwise, the gas injection pressure needs to be increased to mobilize the oil column remaining in the pores. When the critical pore radius is exceeded, it still needs to be higher than the minimum oil column height to realize FFGD. At the same oil column height, with the decrease of GOC migration rate, the smaller pore throats can be mobilized by FFGD. The smaller the GOC migration rate, the smaller the viscous force. Gravity force plays a dominant role in the fluid flow, and it helps to mobilize the residual oil in small pores. This condition, however, can only appear in the high-permeability layer.

The minimum oil column height required for FFGD under different pore radius conditions is calculated by Eq. (7), as shown in Fig. 3. The results illustrate that the oil in the pores with 0.16 μm diameter can be mobilized by FFGD when the GOC migration rate is greater than 0.001 m/d and the height of the oil column is greater than 478.5 m, but this condition is basically impossible. In pores greater than 10 μm in diameter, the minimum oil column height is basically not affected by the change of the GOC migration rate, and the oil in the pores can be driven by FFGD when the oil column is longer than 0.32∼0.42 m. The longer the remaining oil column, the smaller the pore radius that will be mobilized by gravity force. In addition, the longer the continuous oil column, the greater the gravity of the oil column, the more obvious the effect of its own gravity, and the easier it will be to overcome the capillary force and the viscous force, i.e., smaller pores can be utilized. This is in agreement with the observation that, in the early stage of reservoir development, the length of the continuous oil column is large, and the oil column in most of the pores can migrate by gravity. However, at the end of water injection (or gas injection) in the process, the length of the remaining oil column in the pores is small, and only the oil columns in fractures and ultra-high permeability channels can migrate by gravity alone.

3. Characteristics of gas-oil contact during GAGD

3.1 Gas-oil contact calculation model

The GOC is a form of oil-gas transition zone during GAGD (Rao et al., 2004; Chen et al., 2020; Kong et al., 2020), and it moves steadily towards the oil well. The classic capillary model generally assumes that the rock in the actual reservoir is composed of multiple capillary tubes with unequal diameters (Purcell, 1949; Wall and Brown, 1981), as shown in Fig. 4. The characteristics of GOC are analyzed based on the capillary model. It is assumed that the dissolution of gas in crude oil and the immiscibility of the two phases are ignored, the gas is compressible fluid and the oil is incompressible fluid during GAGD. Considering the density difference between oil and gas and the inclination of capillary tubes (gravity domination), the capillary model is simplified into two parallel capillary tubes (TT1 and TT2) with unequal diameters, r_1 and r_2 respectively represent the radius of TT1 and TT2, as shown in Fig. 5.

When analyzing the forces of the oil column in the motion direction, the resultant force of the oil column in TT1 and TT2 can be obtained by Eq. (6). The resultant force of Gas$_1$ p_{F1} in TT1 can be obtained as:

$$p_{F1} = p_{1g} - p_{2o} + \rho_g g h \sin\alpha - \frac{2\sigma\cos\theta_1}{r_1} - \frac{8\mu_g v_1 h}{r_1^2} \quad (9)$$

where p_{1g} and p_{2o} respectively represent the gas phase pressure in TT1 and the oil phase pressure in TT2 at the GOC, h denotes the height difference between TT1 and TT2, θ_1 represents the wetting angle in TT1, and v_1 denotes the gas velocity rate in TT1.

Table 2. Physical properties and pore structure characteristics of Jilin oilfield core.

Parameter	Permeability ($\times 10^{-3}$ μm^2)	Porosity (%)	Pore Radius (μm)		
			Maximum	Average	Median
Value	204	25.5	10.577	4.409	2.428

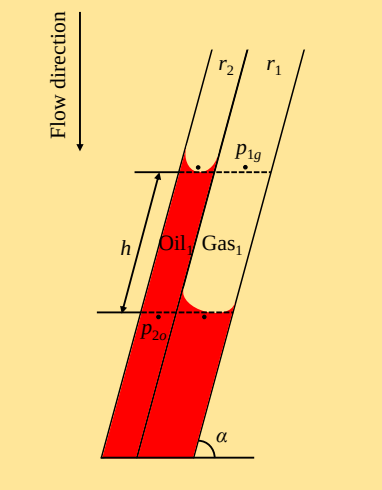

Fig. 5. Schematic diagram of unequal-diameter parallel capillary model (Right: TT1; Left: TT2).

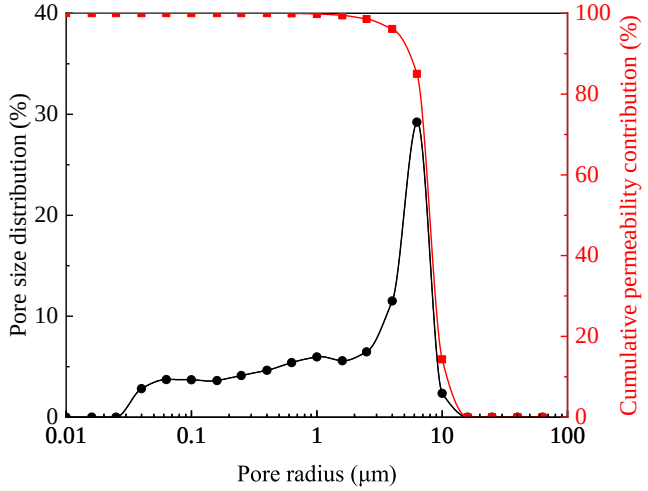

Fig. 6. Pore size distribution and cumulative permeability contribution of Jilin oilfield core.

The resultant force of Oil_1 p_{F2} in TT2 can be calculated by:

$$p_{F2} = p_{1g} - p_{2o} + \rho_o g h \sin\alpha - \frac{2\sigma\cos\theta_2}{r_2} - \frac{8\mu_o v_2 h}{r_2^2} \quad (10)$$

where θ_2 represents the wetting angle in TT2, and v_2 denotes the gas velocity rate in TT2.

The oil-gas transition zone moves steadily towards the oil well during GAGD. In other words, it does not change, that is, the movement of Oil_1 and Gas_1 in two parallel capillaries is relatively static. Thus, the force and the migration rate remain the same, i.e., $p_{F1} = p_{F2}$, $v_1 = v_2 = v$. When Eqs. (9) and (10) are merged, the height difference between TT1 and TT2 can be obtained by Eq. (11), as shown below. Therefore, Eq. (11) can be used to calculate the height difference of GOC in each capillary according to the capillary model, that is, the height of the GOC. This refers to the gas front location based on the maximum pore, which characterizes the migration law of the oil-gas transition zone.

$$h = \frac{2\sigma\left(\frac{\cos\theta_2}{r_2} - \frac{\cos\theta_1}{r_1}\right)}{8v\left(\frac{\mu_g}{r_1^2} - \frac{\mu_o}{r_2^2}\right) + (\rho_o - \rho_g)g\sin\alpha} \quad (11)$$

The numerator of Eq. (11) is always greater than 0, so its denominator should also be greater than 0, which can be obtained as:

$$8v\left(\frac{\mu_g}{r_1^2} - \frac{\mu_o}{r_2^2}\right) + (\rho_o - \rho_g)g\sin\alpha > 0 \quad (12)$$

From Eq. (12), when the large pore radius r_1 is known, there is a mobilization limit of pore radius r_2 at a certain GOC migration rate, and the mobilization limit of pore radius r_2 can be calculated as:

$$r_2 > \sqrt{\frac{8v\mu_o}{\frac{8v\mu_g}{r_1^2} + (\rho_o - \rho_g)g\sin\alpha}} \quad (13)$$

3.2 Effect of GOC migration rate

Here, the mercury injection capillary pressure data are used to quantify the pore size distribution (PSD) of the core. The representative core parameters of Jilin Oilfield are selected to calculate the characteristics of gas-oil contact, and its pore radius distribution is shown in Fig. 6 and Table 2. It can also be seen from Table 2 that the maximum pore radius is 10.577 μm.

Based on the capillary model, rock is composed of multiple capillary tubes with unequal diameters (Purcell, 1949; Wall and Brown, 1981), similar to the PSD. The gas front location at different pore radii can be calculated by Eq. (11) combining the fluid parameters in Table 1, and based on the maximum pore radius $r_1 = 10.577$ μm.

The pore scale oil mobilization limit can be obtained by Eq. (13), and Fig. 7 shows the mobilization limit of pore radius r_2 at different GOC migration rates based on $r_1 = 10.577$ μm. It is illustrated that the pore radius limit mobilization by GAGD decreases with the reduction of GOC migration rate. When the GOC migration rate is 1 m/d, the pores with a radius larger than 4.95 μm can be driven by GAGD. Meanwhile, when the GOC migration rate is reduced to 0.001 m/d, the pores with a radius larger than 0.16 μm can be driven during GAGD. The viscous force is proportional to the GOC migration rate; the smaller the viscous force, the greater the gravity drainage, and the smaller pores are to be involved in mobilization.

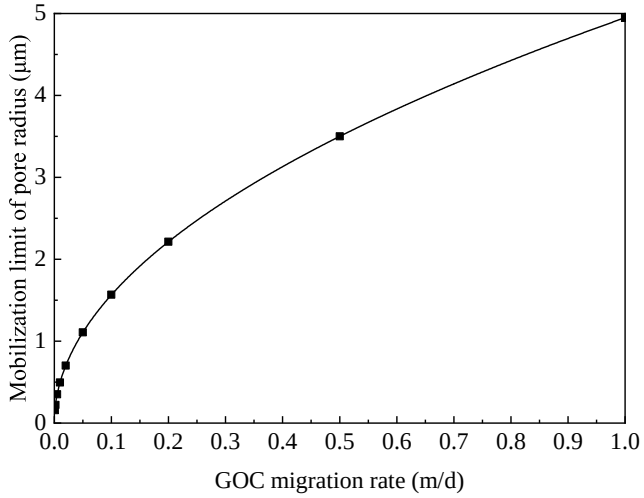

Fig. 7. Mobilization limit of pore radius r_2 at different GOC migration rates.

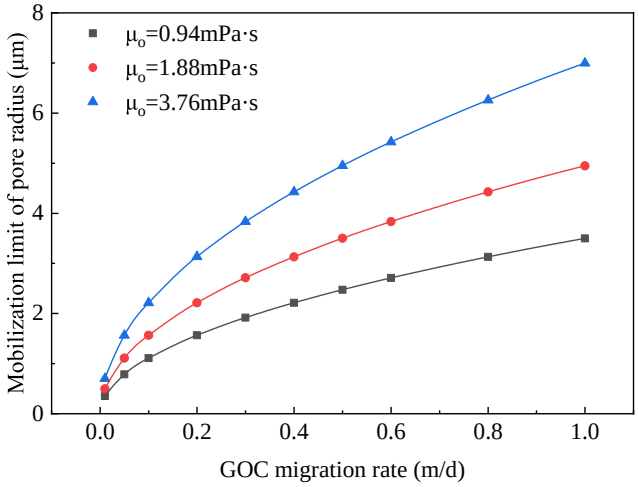

Fig. 9. Mobilization limit of pore radius r_2 under different oil viscosities.

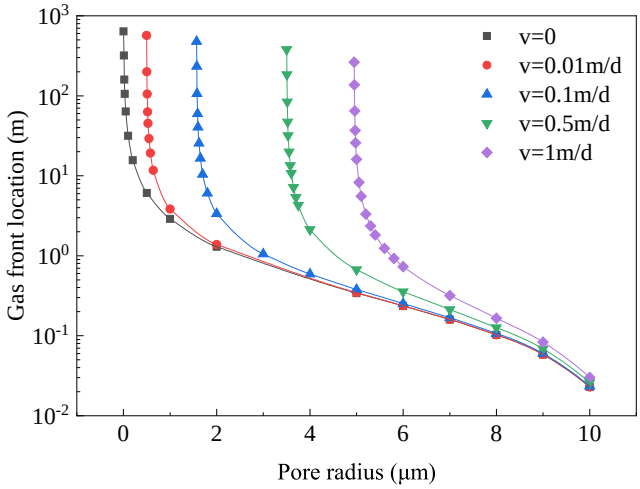

Fig. 8. Gas front location based on $r_1 = 10.577$ μm at different pore radii under different GOC migration rates.

The gas front location based on $r_1 = 10.577$ μm at different pore radii under different GOC migration rates are calculated according to Eq. (11), as shown in Fig. 8. It is revealed that the gas front location difference increases as the pore radius decreases under the same GOC migration rate. The difference in capillary force and viscous force for different pore radii causes the GOC to occur in the form of a transition zone. When the GOC migration rate is 0.01 m/d, the gas front location in the pore with a radius of 0.5 μm is 325.89 m, while that in the pore with a radius of 10 μm is only 0.023 m. That is, premature gas breakthrough occurs earlier in pores with a radius of 10 μm than pores with a radius of 0.5 μm, which is caused by smaller capillary force and viscous force. When the gas breaks through, the oil flow in the macropores is dominated by film flow, while the flow in small pores is dominated by gravity drainage that overcomes capillary force and viscous force. When the pore radius is greater than 10 μm, the gas front location difference does not change significantly with the change of GOC migration rate. The smaller the GOC migration rate, the larger the transition zone. When the GOC migration rate is 0, the viscous force disappears and the height of GOC is the largest, which is consistent with the shape of the original GOC.

3.3 Effect of oil viscosity

Here, the GOC characteristics the during GAGD under different oil viscosities are investigated. Fig. 9 shows the mobilization limit of pore radius r_2 at different oil viscosities. The injected gas has the general effect of reducing the viscosity of the crude oil. It can be found that the mobilization limit of pore radius r_2 is reduced from 1.57 to 1.11 μm as the oil viscosity decreases from 1.88 to 0.94 mPa·s when the GOC migration rate is 0.1 m/d. With long-term gas injection development, the oil viscosity increases. The mobilization limit of pore radius r_2 is 2.21 μm when the oil viscosity increases to 3.76 mPa·s. The viscous force as a form of resistance increases with the increase in oil viscosity. At a certain gas injection velocity, the lower the crude oil viscosity, the easier it is to utilize a smaller pore throat. Meanwhile, lower crude oil viscosity can reduce the flow ratio, effectively inhibit the viscous fingering effect and stabilize the displacement front, delay the gas breakthrough and extend the gas production rate, ultimately improving the GAGD recovery. Therefore, as the oil viscosity increases, the swept pore volume by GAGD becomes smaller, and the GAGD development effect becomes impaired.

As shown in Fig. 10, the GOC characteristics are similar under different oil viscosities. The gas front location difference and GOC transition zone increase with the rise of oil viscosity. The higher the oil viscosity, the more difficult to mobilize the oil in the smaller pores and the larger the difference between the viscosity of gas and oil, which leads to the formation of viscous fingering, causing the instability of the displacement front, which in turn will reduce the swept volume and the recovery degree. The increase of oil viscosity affects the development effect in the later stage of GAGD. Therefore, the GAGD process is more suitable for low-viscosity reservoirs.

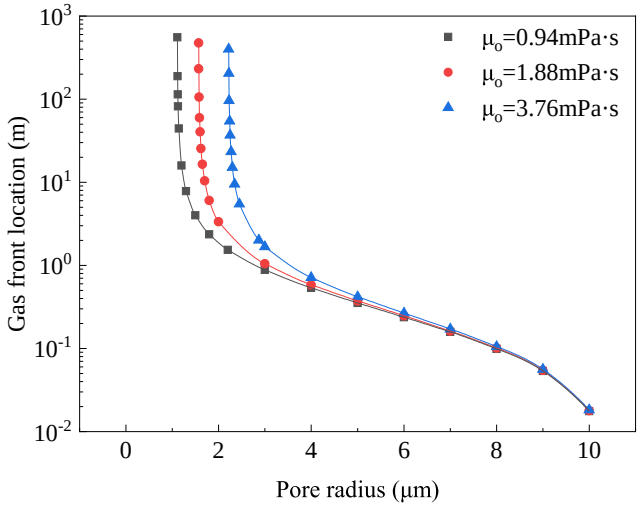

Fig. 10. Gas front location based on $r_1 = 10.577$ μm at different pore radii under different oil viscosities ($v = 0.1$ m/d).

4. Determination of critical gas injection rate

The maximum pore radius r_1 can also be obtained by PSD. If the minimum pore radius r_2 is known, the maximum GOC migration rate can be calculated by Eq. (14), which is transformed as:

$$v = \frac{(\rho_o - \rho_g) g \sin\alpha}{\frac{8\mu_o}{r_2^2} - \frac{8\mu_g}{r_1^2}} \tag{14}$$

Here, the critical gas injection rate can be determined by the maximum GOC migration rate. The main problem is how to determine the minimum pore radius. In general, the contribution of differently sized pore throats to reservoir permeability is different; the larger the pore throat radius, the greater its contribution to flow capacity. Therefore, the mainstream pore throat radius is defined here as the weighted average of all pore-throats for a cumulative permeability contribution of 99.9%, and can be calculated from the mercury injection capillary pressure data (Gao et al., 2021). The mainstream pore-throat radius can more accurately reflect the reservoir flow capacity, which relates the macroscopic flow capacity of the reservoir to the microscopic pore structure characteristics parameters. The potential of gas injection development depends on the distribution of macropores, which are the main contributors to reservoir permeability. Therefore, the mainstream pore-throat radius is the minimum pore radius r_2.

As seen in Fig. 6, the minimum pore radius r_2 of cores from Jilin oilfield is 0.348 μm. The critical gas injection velocity calculated by Eq. (14) is 0.0049 m/d, which is converted to an injected gas volume flow rate of 0.043 mL/min. Chen's experimental results showed that the critical value of gas injection rate for GAGD stabilization displacement is 0.05~0.10 mL/min (Chen et al., 2020). The error between the calculation and the experimental results is relatively insignificant, which confirms the accuracy of the method of this paper. The reason is mainly that, in this work, the interaction between gas and crude oil, such as crude oil oxidation and viscosity reduction, is not considered in the calculation. Although the critical gas injection rate can mobilize the mainstream pore throats, the oil displacement efficiency will not be too high due to the connectivity of individual pores and the entrapment of oil in the reality reservoir. At the critical injection rate, the gas injection efficiency period can be increased, but this affects the economic benefits. In practice, it is necessary to additionally optimize the gas injection rate by considering the economic benefits based on the critical injection rate.

5. Conclusions

1) Driven pressure difference and gravity are the driving forces for displacing oil, whereas capillary force and viscous force are the resistance forces during GAGD. FFGD can be realized when the critical GOC migration rate, critical pore radius and oil column height are exceeded. Otherwise, the gas injection pressure needs to be increased to mobilize the oil column remaining in the pores. The optimization of gas injection rate and oil viscosity reduction can increase the stable production time and promote the stabilization of GAGD.
2) Differences in the capillary force and viscous force of different pore radii cause the GOC existing in the form of a transition zone. When the gas breaks through the macropores, the oil flow is dominated by film flow in such pores, while the flow in small pores is dominated by gravity drainage that overcomes capillary force and viscous force. The pore radius limit mobilization by GAGD decrease with the reduction of GOC migration rate. Otherwise, the smaller the GOC migration rate, the larger the transition zone.
3) A method for determining the critical gas injection rate considering micropore heterogeneity is established based on the capillary model. Based on this method, the critical gas injection velocity is selected from 0.0049 m/d for the Jilin oilfield, which can satisfy the stable displacement conditions while mobilizing the mainstream pore throats.

Acknowledgement

The authors acknowledge the financial support from the Natural Sciences for Youth Foundation of China (No. 42102163) and the Fundamental Research Funds of the Central Universities (No. FRF-TP-20-006A1).

Conflict of interest

The authors declare no competing interest.

References

Al-Mudhafar, W. J., Rao, D., McCreery, E. Evaluation of immiscible CO_2 enhance oil recovery through the CGI, WAG, and GAGD processes in south rumaila oil field. Paper We P2 06 Presented at 79th EAGE Conference and Exhibition, Paris, France, 12-15 June, 2017.

Chen, X., Li, Y., Liao, G., et al. Experimental investigation on stable displacement mechanism and oil recovery enhancement of oxygen-reduced air assisted gravity drainage. Petroleum Exploration and Development, 2020, 47(4): 836-845.

Colla, P. A new analytical method for the motion of a two-phase interface in a tilted porous medium. Paper SGP-TR-202 Presented at 39th Stanford Geothermal Workshop, Stanford University, Stanford, California, USA, 24-26 February, 2014.

Dake, L. P. Fundamentals of Reservoir Engineering. Amsterdam, Netherlands, Elsevier, 1978.

Dietz, D. A theoretical approach to the problem of encroaching and by-passing edge water. Proc, 1953, 56: 83-92.

Dumore, J. M. Stability considerations in downward miscible displacements. Society of Petroleum Engineers Journal, 1964, 4(4): 356-362.

Gao, W., Li, Y., Zhang, J., et al. Effect of surfactant on pore-scale mobilization characteristics in various pore structure conglomerate for enhanced oil recovery. Colloids and Surfaces A: Physicochemical and Engineering Aspects, 2021, 627: 127150.

Grattoni, C. A., Jing, X. D., Dawe, R. A. Dimensionless groups for three-phase gravity drainage flow in porous media. Journal of Petroleum Science and Engineering, 2001, 29(1): 53-65.

Hagoort, J. Oil recovery by gravity drainage. Society of Petroleum Engineers Journal, 1980, 20(3): 139-150.

Hasanzadeh, M., Azin, R., Fatehi, R., et al. New insights into forced and free fall gravity drainage performance in a fractured physical model. Journal of Petroleum Science and Engineering, 2021, 203: 108568.

Khorshidian, H., James, L. A., Butt, S. D. Demonstrating the effect of hydraulic continuity of the wetting phase on the performance of pore network micromodels during gas assisted gravity drainage. Journal of Petroleum Science and Engineering, 2018, 165: 375-387.

Kong, D., Gao, Y., Sarma, H., et al. Experimental investigation of immiscible water-alternating-gas injection in ultra-high water-cut stage reservoir. Advances in Geo-Energy Research, 2021a, 5(2): 139-152.

Kong, D., Lian, P., Zheng, R., et al. Performance demonstration of gas-assisted gravity drainage in a heterogeneous reservoir using a 3D scaled model. RSC Advances, 2021b, 11(49): 30610-30622.

Kong, D., Lian, P., Zhu, W., et al. Pore-scale investigation of immiscible gas-assisted gravity drainage. Physics of Fluids, 2020, 32(12): 122004.

Kulkarni, M. M., Rao, D. N. Analytical modeling of the forced gravity drainage GAGD process. Paper 72361 Presented at AIChE Annual Meeting, San Francisco, CA, USA, 12-17 November, 2006.

Liu, Z., Yang, Y., Yao, J., et al. Pore-scale remaining oil distribution under different pore volume water injection based on CT technology. Advances in Geo-Energy Research, 2017, 1(3): 171-181.

Lv, B., Ma, Q., Cheng, H. Simulation research on CO_2 and water flooding of long core test. Natural Gas and Oil, 2015, 33(2): 69-72. (in Chinese)

Mahmoud, T., Rao, D. N. Mechanisms and performance demonstration of the gas-assisted gravity-drainage process using visual models. Paper SPE 110132 Presented at SPE Annual Technical Conference and Exhibition, Anaheim, California, USA, 11-14 November, 2007.

Meszaros, G., Chakma, A., Jha, K., et al. Scaled model studies and numerical simulation of inert gas injection with horizontal wells. Paper SPE 20529 Presented at SPE Annual Technical Conference and Exhibition, New Orleans, LA, USA, 23-26 September, 1990.

Namba, T., Nakashima, T., Yonebayashi, H., et al. Force balance analysis and efficient measures to improve vertical sweep efficiency in oil-wet carbonate reservoirs. Paper SPE 193099 Presented at Abu Dhabi International Petroleum Exhibition and Conference, Abu Dhabi, UAE, 12-15 November, 2018.

Outmans, H. D. Transient interfaces during immiscible liquid-liquid displacement in porous media. Society of Petroleum Engineers Journal, 1962, 2(2): 156-164.

Purcell, W. R. Capillary pressures—their measurement using mercury and the calculation of permeability therefrom. Journal of Petroleum Technology, 1949, 1(2): 39-48.

Raeini, A. Q., Blunt, M. J., Bijeljic, B. Direct simulations of two-phase flow on micro-CT images of porous media and upscaling of pore-scale forces. Advances in Water Resources, 2014, 74: 116-126.

Rahman, A., Happy, F. A., Ahmed, S., et al. Development of scaling criteria for enhanced oil recovery: A review. Journal of Petroleum Science and Engineering, 2017, 158: 66-79.

Rao, D., Ayirala, S., Kulkarni, M., et al. Development of gas assisted gravity drainage (GAGD) process for improved light oil recovery. Paper SPE 89357 Presented at SPE/DOE Symposium on Improved Oil Recovery, Tulsa, Tulsa, Oklahoma, 17-21 April, 2004.

S. Hill, M. A., F. Inst. P., F. S. S. Channeling in packed columns. Chemical Engineering Science, 1952, 1(6): 247-253.

Sheldon, J. W., Fayers, F. J. The motion of an interface between two fluids in a slightly dipping porous medium. Society of Petroleum Engineers Journal, 1962, 2(3): 275-282.

Stephen, K. D., Pickup, G. E., Sorbie, K. S. The local analysis of changing force balances in immiscible incompressible two-phase flow. Transport in Porous Media, 2001, 45(1): 63-88.

Wall, G., Brown, R. The determination of pore-size distributions from sorption isotherms and mercury penetration in interconnected pores: The application of percolation theory. Journal of Colloid and Interface Science, 1981, 82(1): 141-149.

Wang, J., Ji, Z., Liu, H., et al. Experiments on nitrogen assisted gravity drainage in fractured-vuggy reservoirs. Petroleum Exploration and Development, 2019, 46(2): 355-366.

Yu, H., Wang, L., Zhou, D., et al. Experimental study on sweep characteristics of gas gravity drainage in the interlayer oil reservoir. Frontiers in Energy Research, 2021, 9: 760315.